

MARLIN: Multi-Agent Reinforcement Learning with Murmuration Intelligence and LLM Guidance for Reservoir Management

Heming Fu^{1*}, Guojun Xiong^{2*}, Jian Li¹, Shan Lin¹

¹Stony Brook University, ²Harvard University

{heming.fu, jian.li.3, shan.lin}@stonybrook.edu, gjxiong@g.harvard.edu

ABSTRACT

As climate change intensifies extreme weather events, water disasters pose growing threats to global communities, making adaptive reservoir management critical for protecting vulnerable populations and ensuring water security. Modern water resource management faces unprecedented challenges from cascading uncertainties propagating through interconnected reservoir networks. These uncertainties, rooted in physical water transfer losses and environmental variability, make precise control difficult. For example, sending 10 tons downstream may yield only 8-12 tons due to evaporation and seepage. Traditional centralized optimization approaches suffer from exponential computational complexity and cannot effectively handle such real-world uncertainties, while existing multi-agent reinforcement learning (MARL) methods fail to achieve effective coordination under uncertainty. To address these challenges, we present MARLIN, a decentralized reservoir management framework inspired by starling murmurations intelligence. Integrating bio-inspired *alignment*, *separation*, and *cohesion* rules with MARL, MARLIN enables individual reservoirs to make local decisions while achieving emergent global coordination. In addition, a LLM provides real-time reward shaping signals, guiding agents to adapt to environmental changes and human-defined preferences. Experiments on real-world USGS data show that MARLIN improves uncertainty handling by 23%, cuts computation by 35%, and accelerates flood response by 68%, exhibiting super-linear coordination, with complexity scaling $5.4\times$ from 400 to 10,000 nodes. These results demonstrate MARLIN’s potential for disaster prevention and protecting communities through intelligent, scalable water resource management.

1 INTRODUCTION

Water resource management is at a critical inflection point, as traditional engineering approaches are increasingly inadequate for the complexity and uncertainty of modern hydrological systems. Climate change has dramatically altered

precipitation patterns (see Figure 1c), resulting in more frequent and severe extreme weather events that disproportionately impact vulnerable populations. The consequences are global: between 2000 and 2019, floods affected over 1.65 billion people and caused an estimated 651 billion in economic losses [38], while droughts impacted 1.43 billion people and resulted in damages exceeding 130 billion [5]. Events that were once considered century-scale extremes now occur every 20 years in many regions, and flash flood frequency has surged by 21% over the past decade [20].

Recent disasters underscore the urgent need for adaptive water management systems. The 2021 European floods resulted in over 200 deaths and approximately €50 billion in damages, with critical infrastructure and institutional coordination across jurisdictions proving inadequate during the response [7]. New York’s 2023 extreme rainfall events exposed critical infrastructure vulnerabilities, affecting millions in subway systems and low-lying communities [17]. Texas winter storms continue to threaten water security for vulnerable populations when power-dependent pumping systems fail [6, 28]. Meanwhile, in the U.S., Lake Mead and Lake Powell have dropped below 30% capacity amid a megadrought, threatening water supplies for 40 million people [1, 3]. A recent systematic study analyzed over 550 dam failure cases across the United States and found that current hydrologic design standards and reservoir operation protocols are often inadequate for managing clustered rainfall and other extreme events. These limitations have been linked to a series of cascading failure incidents, including the 2020 Michigan dam breach and the 2017 Oroville spillway collapse, both regarded as emblematic of systemic vulnerabilities. Together, they highlight the deeper risks posed by fragmented dam oversight and insufficient hydrological response mechanisms in the U.S. [14].

These failures reveal two key limitations of current approaches. First, as reservoir networks grow, computational complexity scales as $O(n^3)$ (due to pairwise interactions and constraint coupling in optimization), making real-time control impractical, especially since advanced Model predictive control (MPC) systems cannot respond quickly to

* Equal contribution.



Figure 1: Water resource management challenges: (a) complex networks of interconnected reservoirs requiring coordination, (b) individual reservoirs must be locally managed, and (c) high global flood frequency demanding robust management systems.

fast-changing conditions [16, 19, 33]. Second, cascading uncertainty amplifies prediction errors in centralized models. We identify a dual-layer structure: **Level 1** uncertainty arises from the water transfer process itself (e.g., sending 10 tons downstream may yield 8–12 tons due to evaporation, seepage, and variable channel conditions); **Level 2** stems from variable environmental factors like rainfall and soil saturation. Small measurement errors (5–10% in flow sensors and level gauges) at individual nodes can compound through network propagation. Assuming independent error propagation with 7% average measurement uncertainty, the cumulative uncertainty grows as $\sigma_{cumulative} = \sigma_{base} \sqrt{n}$, reaching approximately 22% after 10 cascaded links, which can exceed 40% under correlated environmental conditions, rendering centralized control unreliable.

Multi-agent reinforcement learning (MARL) provides a distributed alternative but remains vulnerable to uncertainty [12, 24, 36, 39], which often suffer from training instability and poor convergence under cascading uncertainties, resulting in unsafe, oscillatory behaviors in practice [11]. In contrast, nature demonstrates robust coordination through simple local rules. Starling murmurations (Figure 2) show how thousands of individuals achieve complex, adaptive organization through alignment, separation, and cohesion—without centralized control [2, 13, 25]. These principles support rapid, resilient coordination even in noisy and uncertain environments.

Inspired by these natural mechanisms, we introduce MARLIN, a decentralized framework that integrates bio-inspired coordination with reinforcement learning for managing complex water systems under dual-layer uncertainty. MARLIN features three key components: (1) murmuration-inspired



Figure 2: Starling Murmuration: emergent intelligence from simple local coordination rules.

rules that map alignment, separation, and cohesion to reservoir control actions, specifically designed to handle Level 1 water transfer uncertainties while fostering local responsiveness and global safety; (2) a specialized MARL architecture that incorporates these coordination signals into policy gradients for stable multi-agent learning; and (3) To address Level 2 environmental uncertainties, which involve complex interactions between weather patterns, regulatory policies, and stakeholder priorities that cannot be easily encoded in mathematical models, we integrate LLM that can process diverse textual information (weather forecasts, regulatory documents, stakeholder communications) and translate this heterogeneous knowledge into appropriate reward shaping, enabling the system to adapt to changing environmental and social contexts that would be difficult to capture through traditional optimization approaches.

Experiments on real-world USGS watershed data demonstrate that MARLIN improves uncertainty handling by 23%, reduces computation by 35%, speeds up flood response by 68%, and improves regional water balance by 42% compared to state-of-the-art baselines.

In summary, our main contributions are:

- ▶ We propose the first bio-inspired MARL framework that applies starling murmuration principles to decentralized water resource management, where complex system-wide coordination emerges naturally from simple local interactions, scaling effectively to thousands of agents.
- ▶ We design a dual-layer uncertainty handling mechanism, where local coordination rules (alignment, separation, cohesion) address water transfer uncertainty, and LLM-guided reward shaping adapts to environmental fluctuations and human preferences.
- ▶ We validate our approach on real-world USGS data, demonstrating 23% improvement in uncertainty handling, 35% reduction in computation, and super-linear

scalability with increasing system size and coordination complexity, with significant potential for protecting vulnerable communities from water-related disasters.

2 RELATED WORK

Water Management and Multi-Agent Systems. Classical water management relied on deterministic optimization like dynamic programming [18, 35] and network flow models [30], suffering from exponential complexity and static assumptions. MPC became dominant in operational systems but demonstrates critical limitations during rapid changes. The 2011 Mississippi floods exemplified delayed recalibration contributing to \$2.8 billion avoidable damage [27]. MARL emerged as a distributed alternative. MADDPG [21] uses centralized critics with decentralized actors, QMIX [24] employs value decomposition with monotonic mixing, and MAPPO [36] adapts PPO to multi-agent settings. However, these methods face training instability under non-stationary environments and assume coordination emerges naturally from individual optimization, overlooking explicit coordination mechanisms needed for uncertainty handling [8].

Bio-Inspired Coordination. Reynolds formalized flocking behavior into alignment, separation, and cohesion rules [25]. Theoretical analysis revealed phase transitions between ordered and disordered states [4, 32], while empirical studies confirmed scale-free correlations and rapid information propagation [2]. These inspired algorithms like Particle Swarm Optimization [15] and practical swarm robotics applications [23, 26]. However, most focus on continuous motion rather than discrete decision-making required in infrastructure control. **LLMs for Adaptive Control.** Recent work explores LLMs for reward design and adaptation [31, 34]. Eureka [22] uses GPT-4 for automated reward generation, while L2R [9, 10] enables natural language reward specification. However, these approaches primarily focus on single-agent settings or assume full observability, limiting their applicability in decentralized multi-agent systems.

3 PROBLEM FORMULATION

Modern water resource management systems face unprecedented challenges from cascading uncertainties that propagate through interconnected reservoir networks. We formulate this as a distributed coordination problem under dual-layer uncertainty, where traditional centralized approaches fail due to exponential computational complexity and compounding prediction errors.

3.1 Network Model and Stochastic Dynamics

We model the reservoir network as a time-varying stochastic graph $\mathcal{G}(t) = (\mathcal{V}, \mathcal{E}, \Theta(t))$, where $\mathcal{V} = \{v_1, v_2, \dots, v_n\}$ represents the set of n reservoir nodes; $\mathcal{E} \subseteq \mathcal{V} \times \mathcal{V}$ denotes water flow channels between reservoirs; and $\Theta(t) = \{\theta_1(t), \theta_2(t), \dots, \theta_m(t)\}$ captures time-varying environmental parameters. Each reservoir i maintains state vector $\mathbf{s}_i(t) = [h_i(t), q_{\text{in},i}(t), q_{\text{out},i}(t), \mathbf{w}_i(t), \xi_i(t)]^\top$, where $h_i(t)$ is water level, $q_{\text{in}/\text{out},i}(t)$ represent flows, $\mathbf{w}_i(t)$ captures weather, and $\xi_i(t)$ represents demand patterns. The water level dynamics follow a stochastic differential equation:

$$\frac{dh_i(t)}{dt} = \frac{1}{C_i} \left[\sum_{j \in \mathcal{N}_{\text{in}}(i)} f_{ji}(t) - \sum_{k \in \mathcal{N}_{\text{out}}(i)} f_{ik}(t) + q_{\text{ext},i}(t) + \eta_i(t) \right], \quad (1)$$

where C_i is reservoir capacity, $f_{ij}(t)$ represents actual water transfer (subject to uncertainty), $q_{\text{ext},i}(t)$ captures external inflows, and $\eta_i(t) \sim \mathcal{N}(0, \sigma_{\eta,i}^2)$ models stochastic noise.

3.2 Dual-Layer Uncertainty Framework

The critical challenge lies in cascading uncertainty amplification. We identify two distinct sources:

Level 1: Water Transfer Uncertainty arises from physical losses and cascading effects during water transport. When reservoir i releases volume $a_i(t)$, the actual received volume follows:

$$f_{ij}(t) \sim \mathcal{N}(\mu_{ij}(t), \sigma_{ij}^2(t)), \\ \mu_{ij}(t) = \alpha_{ij}(t) \cdot g_{ij}(a_i(t), h_i(t), h_j(t)),$$

where $\alpha_{ij}(t) \in [0, 1]$ represents channel efficiency (accounting for evaporation, seepage) and $g_{ij}(\cdot)$ is the nominal flow function.

Level 2: Environmental Parameter Uncertainty captures how environmental conditions affect system parameters:

$$\sigma_{ij}^2(t) \sim \text{Gamma}(\kappa_{ij}, \theta_{ij}(t)), \\ \theta_{ij}(t) = \theta_{\text{base},ij} + \beta_{\text{environment}} \|\mathbf{w}_i(t) - \mathbf{w}_j(t)\|_2,$$

meaning uncertainty increases with environmental changes caused by weather or human activities between connected reservoirs, reflecting how environmental variability affects transfer reliability.

3.3 Multi-Objective Control Problem

Water management requires balancing competing objectives across spatial and temporal scales. We define:

$$\begin{aligned}
 J_{\text{safety}}(\pi) &= -\mathbb{E}_{\pi} \left[\sum_{t=0}^T \sum_{i=1}^n \lambda_{\text{flood},i} \max(0, h_i(t) - h_{\text{safe},i})^2 \right], \\
 J_{\text{supply}}(\pi) &= \mathbb{E}_{\pi} \left[\sum_{t=0}^T \sum_{i=1}^n \sum_{d \in \mathcal{D}_i} \mathbb{I}[q_{\text{supply},d}(t) \geq q_{\text{demand},d}(t)] \right], \\
 J_{\text{ecology}}(\pi) &= \mathbb{E}_{\pi} \left[\sum_{t=0}^T \min \left(1, \frac{Q_{\text{actual}}(t)}{Q_{\text{eco}}(t)} \right) \right], \\
 J_{\text{efficiency}}(\pi) &= -\mathbb{E}_{\pi} \left[\sum_{t=0}^T \sum_{i=1}^n (c_{\text{op},i} a_i(t) + c_{\text{dev},i} |h_i(t) - h_{\text{target},i}|^2) \right],
 \end{aligned}$$

where J_{safety} penalizes flood risk (water levels exceeding safe thresholds), J_{supply} measures demand satisfaction rate across all demand points, J_{ecology} ensures ecological flow requirements, and $J_{\text{efficiency}}$ minimizes operational costs and deviations from target levels. Q denotes the flow amounts and c is constant weight. The goal is to find a policy π for the following optimization problem:

$$\begin{aligned}
 \max_{\pi} \quad & \mathbf{J}(\pi) = [J_{\text{safety}}(\pi), J_{\text{supply}}(\pi), J_{\text{ecology}}(\pi), J_{\text{efficiency}}(\pi)]^{\top} \\
 \text{s.t.} \quad & h_{\min,i} \leq h_i(t) \leq h_{\max,i}, \quad \forall i \in \mathcal{V}, t, \\
 & \mathbb{P}[h_i(t) > h_{\text{flood},i}] \leq p_{\text{risk}},
 \end{aligned} \tag{2}$$

subject to physical capacity constraints and probabilistic flood risk limits.

3.4 Distributed Control Challenge

Each agent i operates under partial observability with local information:

$$\mathcal{O}_i(t) = \{\mathbf{s}_i(t), \{\hat{\mathbf{s}}_j(t - \tau_j)\}_{j \in \mathcal{N}_i}, \mathbf{w}_{\text{forecast},i}(t:t+H)\}, \tag{3}$$

including delayed neighbor states and weather forecasts. The challenge is finding decentralized policies $\{\pi_i : \mathcal{O}_i \rightarrow \mathcal{A}_i\}_{i=1}^n$ that achieve global coordination under local constraints. $\mathbf{w}_{\text{forecast},i}(t:t+H)$ provides weather forecasts for the next H hours.

4 METHODOLOGY

MARLIN addresses dual-layer uncertainty through three components: murmuration-inspired coordination, MARL, and LLM-guided adaptive reward shaping. Figure 3 presents MARLIN system design.

4.1 Murmuration-Inspired Coordination Layer

Drawing from starling murmuration, we adapt three coordination rules to reservoir management, where each rule addresses specific coordination challenges:

Adaptive Alignment Rule encourages coordinated release strategies among neighboring reservoirs:

$$\mathcal{L}_{\text{align},i}(t) = \sum_{j \in \mathcal{N}_i} w_{ij}(t) \cdot \|a_i - \bar{a}_{ij}\|^2, \tag{4}$$

where \mathcal{N}_i is the set of neighboring reservoirs that can communicate with reservoir i , a_i is reservoir i 's current release action, \bar{a}_{ij} is the average release action between reservoirs i and j , and $w_{ij}(t)$ are time-varying weights computed as:

$$w_{ij}(t) = \frac{\exp(-\beta_d d_{ij} - \beta_e \|\mathbf{w}_i - \mathbf{w}_j\|_2)}{\sum_{k \in \mathcal{N}_i} \exp(-\beta_d d_{ik} - \beta_e \|\mathbf{w}_i - \mathbf{w}_k\|_2)},$$

Here d_{ij} is the geographic distance between reservoirs, \mathbf{w}_i represents local weather conditions at reservoir i , and β_d, β_e are scaling parameters that control the influence of distance and weather similarity. This rule mimics how starlings align their flight direction with nearby birds. In reservoir management, when California's Central Valley faces drought, this rule ensures upstream reservoirs (like Shasta and Oroville) coordinate their releases to maintain consistent downstream supply rather than acting independently. The weights $w_{ij}(t)$ prioritize coordination with geographically closer neighbors, so reservoirs in the same watershed coordinate more strongly than distant ones.

Strategic Separation Rule maintains beneficial diversity to prevent system-wide failures:

$$\mathcal{L}_{\text{sep},i}(t) = \sum_{j \in \mathcal{N}_i} \phi_{\text{sep}}(\|a_i - a_j\|_2; \tau_i(t), \sigma_i(t)), \tag{5}$$

where $\phi_{\text{sep}}(\cdot)$ is a penalty function that decreases as the difference $\|a_i - a_j\|_2$ increases (encouraging diversity), $\tau_i(t)$ is an adaptive threshold, and $\sigma_i(t)$ controls the penalty strength. The threshold adapts based on local uncertainty:

$$\tau_i(t) = \tau_{\text{base}} \cdot (1 + \alpha_{\tau} \cdot \text{CV}[\{h_j\}_{j \in \mathcal{N}_i}]),$$

where $\text{CV}[\cdot]$ is the coefficient of variation of water levels h_j among neighbors, encouraging more diversity when local conditions are highly variable. Like starlings avoiding collisions by maintaining distance, this rule prevents all reservoirs from making identical decisions. For example, during Texas winter storms, while some reservoirs focus on immediate flood control, others maintain emergency reserves for potential power grid failures. The parameter $\tau_i(t)$ adapts based on local uncertainty—when water levels are highly variable, the system encourages more diverse strategies to avoid cascading failures.

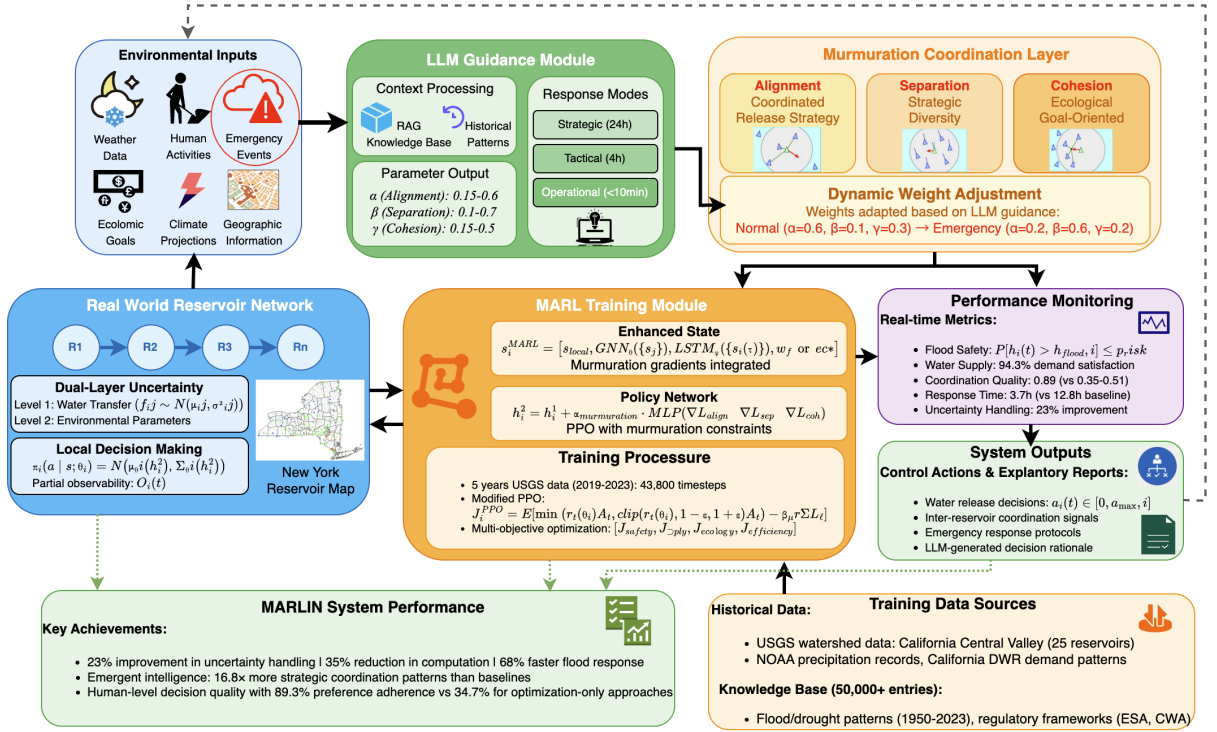


Figure 3: Overview of the MARLIN system architecture and training workflow for distributed reservoir management. The framework integrates bio-inspired coordination with RL in a closed-loop system. Environmental inputs of emergency events (highlighted in red) trigger the LLM Guidance Module to process contextual information and generate dynamic murmuration parameters (α, β, γ). The Murmuration Coordination Layer adaptively applies three bio-inspired rules (Alignment, Separation, Cohesion), shifting weights from normal operations ($\alpha = 0.6, \beta = 0.1, \gamma = 0.3$) to emergency response ($\alpha = 0.2, \beta = 0.6, \gamma = 0.2$). The MARL Training Module incorporates murmuration-based gradients into policy networks via enhanced state representations and modified PPO constraints. Training leverages five years of USGS data and an extensive knowledge base. MARLIN achieves a 23% improvement in uncertainty handling, 35% reduction in computation, 68% faster flood response, and generates 16.8× more strategic coordination patterns than baseline methods.

Ecological Cohesion Rule aligns local actions with system-wide ecological requirements:

$$\mathcal{L}_{coh,i}(t) = \lambda_{eco,i}(t) \cdot \left\| \sum_{j \in \mathcal{P}_i} q_{release,j}(t) - Q_{eco,i}(t) \right\|^2, \quad (6)$$

where \mathcal{P}_i is the set of reservoirs in the same ecological region as i , $q_{release,j}(t)$ is the actual release flow from reservoir j , $Q_{eco,i}(t)$ is the required ecological flow for region i , and $\lambda_{eco,i}(t)$ is a time-varying weight that increases during critical ecological periods (e.g., fish migration seasons). Similar to how starlings maintain flock cohesion, this rule ensures collective reservoir behavior serves global objectives. During salmon migration in the Columbia River, upstream reservoirs coordinate to maintain specific downstream flow patterns despite local agricultural demands, balancing individual reservoir needs with ecosystem requirements.

4.2 MARL with Coordination Integration

Each agent uses enhanced state representation combining multiple information sources:

$$\mathbf{s}_i^{MARL}(t) = \begin{bmatrix} \mathbf{s}_i^{local}(t), GNN_{\theta}(\{\mathbf{s}_j, \mathbf{e}_{ij}\}_{j \in \mathcal{N}_i}), \\ LSTM_{\phi}(\{\mathbf{s}_i(\tau)\}_{\tau=t-K}^t), \mathbf{w}_{forecast,i}(t:t+H) \end{bmatrix}^T.$$

Each component serves a specific purpose:

- 1) $\mathbf{s}_i^{local}(t) = [h_i(t), q_{in,i}(t), q_{out,i}(t)]$ contains local reservoir state (water level, inflows, outflows).
- 2) $GNN_{\theta}(\{\mathbf{s}_j, \mathbf{e}_{ij}\}_{j \in \mathcal{N}_i})$ processes neighbor information, where \mathbf{s}_j are neighbor states and \mathbf{e}_{ij} are edge features (e.g., channel capacity, flow delay between reservoirs i and j).
- 3) $LSTM_{\phi}(\{\mathbf{s}_i(\tau)\}_{\tau=t-K}^t)$ captures historical patterns over past K time steps to identify trends and seasonal patterns.
- 4) $\mathbf{w}_{forecast,i}(t:t+H)$ provides weather forecasts for the next H hours, enabling anticipatory decision-making.

This architecture mimics how starlings process local conditions, observe nearby birds, and anticipate environmental changes. For reservoirs, this means combining local water levels, neighbor reservoir states through GNNs, and weather forecasts to make informed decisions. The policy network integrates murmuration coordination signals:

$$\mathbf{h}_i^{(2)} = \mathbf{h}_i^{(1)} + \alpha_{\text{mur}} \cdot \text{MLP}([\nabla_{a_i} \mathcal{L}_{\text{align}}, \nabla_{a_i} \mathcal{L}_{\text{sep}}, \nabla_{a_i} \mathcal{L}_{\text{coh}}]^\top),$$

where $\mathbf{h}_i^{(1)}$ is the standard policy network hidden state, $\nabla_{a_i} \mathcal{L}_\ell$ are gradients of coordination losses with respect to action a_i , and α_{mur} controls the influence of bio-inspired coordination. These gradients provide directional guidance: alignment gradients push toward neighbor actions, separation gradients push away from identical decisions, and cohesion gradients pull toward global objectives. Such gradients modify the policy’s hidden representation, enabling bio-inspired coordination to emerge naturally during learning without requiring explicit coordination protocols.

We employ modified PPO that balances individual performance with coordination:

$$J_i^{\text{PPO}} = \mathbb{E}_{\mathcal{B}_i} \left[\min(r_t(\theta_i)A_t, \text{clip}(r_t(\theta_i), 1-\epsilon, 1+\epsilon)A_t) \right] - \beta_{\text{mur}} \sum_{\ell \in \{\text{align, sep, coh}\}} \mathcal{L}_{\ell, i}, \quad (7)$$

where \mathcal{B}_i is the experience batch for agent i , $r_t(\theta_i) = \frac{\pi_{\theta_i}(a_t|s_t)}{\pi_{\theta_i^{\text{old}}}(a_t|s_t)}$ is the probability ratio, A_t is the advantage function, and β_{mur} dynamically weights coordination importance. This formulation balances standard PPO performance optimization with murmuration coordination penalties. β_{mur} controls how strongly the bio-inspired rules influence learning. During emergencies, β_{mur} increases to prioritize coordination over individual performance, while in stable periods, it decreases to allow more individual optimization.

4.3 LLM-Guided Adaptive Reward Shaping

To address Level 2 environmental uncertainties involving complex contextual information (weather patterns, regulations, stakeholder preferences), we integrate LLM that process diverse textual information sources like weather reports, regulatory documents, stakeholder communications, and translate this heterogeneous knowledge into appropriate parameter adjustments. We decompose rewards as:

$$R_i = R_{\text{base}, i} + R_{\text{shaped}, i}(\boldsymbol{\psi}(t)),$$

where $R_{\text{base}, i}$ captures standard objectives (safety, supply, efficiency) and $R_{\text{shaped}, i}(\boldsymbol{\psi}(t))$ provides context-aware adjustments based on LLM-processed parameters $\boldsymbol{\psi}(t)$.

The system operates three common coordination modes by adjusting the relative weights of alignment (α), separation (β), and cohesion (γ) rules. The final coordination signal is

computed as:

$$\mathcal{L}_{\text{total}, i}(t) = \alpha \cdot \mathcal{L}_{\text{align}, i}(t) + \beta \cdot \mathcal{L}_{\text{sep}, i}(t) + \gamma \cdot \mathcal{L}_{\text{coh}, i}(t), \quad (8)$$

where $\alpha + \beta + \gamma = 1$ and the weights are dynamically adjusted based on context:

SAC-Alignment (Coordination-First) $\alpha = 0.6, \beta = 0.1, \gamma = 0.3$: Prioritizes coordination for stable periods. During California’s predictable dry season, all Central Valley reservoirs synchronize releases to maintain agricultural water supply while preventing individual depletion.

SAC-Separation (Diversity-First) $\alpha = 0.2, \beta = 0.6, \gamma = 0.2$: Emphasizes diverse strategies for emergency response. During unpredictable Texas winter storms, some reservoirs prioritize immediate flood control while others maintain emergency reserves for potential infrastructure failures.

SAC-Cohesion (Goal-Oriented) ($\alpha = 0.3, \beta = 0.2, \gamma = 0.5$): Focuses on global optimization for ecological protection. During Pacific Northwest salmon migration, upstream reservoirs coordinate to maintain specific flow patterns despite varying local demands.

The LLM processes context at multiple temporal scales:

$$\boldsymbol{\psi}(t) = \begin{cases} \text{LLM}(C_{\text{daily}}, \mathcal{P}_{\text{strategic}}) & \text{Strategic (24h)} \\ \boldsymbol{\psi}_{\text{strategic}} + \Delta\boldsymbol{\psi}_{\text{LLM}}(C_{\text{hourly}}) & \text{Tactical (4h)} \\ \boldsymbol{\psi}_{\text{emergency}} & \text{Operational (10min)} \end{cases}$$

Each temporal scale serves distinct functions:

- 1) **Strategic (24h)**: Processes daily weather reports, seasonal forecasts, and long-term regulatory updates (C_{daily}) along with strategic policies ($\mathcal{P}_{\text{strategic}}$) to set baseline coordination weights for planned operations.
- 2) **Tactical (4h)**: Adds hourly updates (C_{hourly}) such as refined weather forecasts and stakeholder communications to adjust coordination strategy as conditions evolve.
- 3) **Operational (10min)**: Switches to pre-computed emergency parameters ($\boldsymbol{\psi}_{\text{emergency}}$) during critical events when rapid response is essential and there is no time for LLM.

This hierarchical approach enables adaptation from long-term strategic planning (seasonal water allocation) to rapid emergency response (flash flood), matching adaptive coordination strategy to the temporal urgency of the situation.

5 EVALUATION

We conduct two comprehensive experiments to evaluate the effectiveness of MARLIN: (1) assessing the emergence of coordinated behaviors driven by murmuration-inspired mechanisms under uncertainty, and (2) demonstrating the adaptive advantages of LLM-guided reward shaping in dynamic, real-world scenarios.

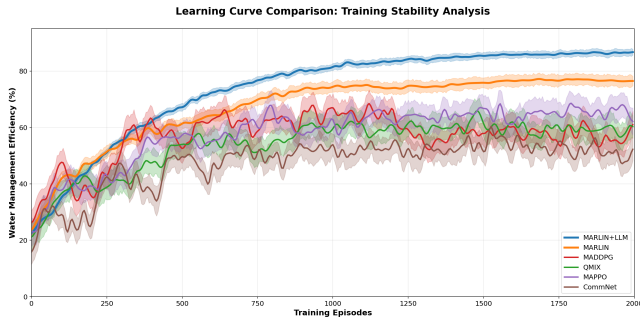


Figure 4: Learning curves demonstrating MARLIN’s stable convergence under dual-layer uncertainty. MARLIN consistently maintains a coefficient of variation below 0.08 during training, while baseline methods show persistent oscillations with $CV > 0.25$. Shaded areas represent the standard deviation across 5 independent runs with different random seeds.

5.1 Experiment 1: Validation of Murmuration-Based Coordination

Setup: We assess the emergence of coordinated behaviors on both the California Central Valley watershed (comprising 25 major reservoirs managing 6.2 million acres of agricultural land) and synthetic networks ranging from 20×20 to 100×100 nodes, under dual-layer uncertainty ($\sigma_{\text{base}} = 0.05$).

Evaluation Metrics: We assess performance across six dimensions: *Coordination Quality*: Measured as the normalized mutual information between agent actions and optimal collective behavior, computed as $Q_c = \frac{1}{n} \sum_{i=1}^n \frac{I(a_i; a_{-i})}{\log n}$, where $I(\cdot; \cdot)$ is mutual information and a_{-i} represents actions of other agents. *Adaptation Speed*: Time to reach 95% of steady-state performance after environmental changes. *Uncertainty Resilience*: Performance retention under varying noise levels (5-15%). *Scalability*: Computational complexity scaling with network size. *Safety*: Percentage of time steps maintaining water levels within safe bounds. *Interpretability*: Rated by practitioners on decision clarity and reasoning transparency.

Models Compared: MARLIN (without LLM integration), MADDPG [21], QMIX [24], MAPPO [37], CommNet [29], and an MPC-Centralized oracle baseline. **Training Data:** Model training utilizes five years of hourly USGS flow measurements (2019–2023; 43,800 timesteps), NOAA precipitation records, and agricultural demand data from the California Department of Water Resources, covering 27 million residents. **Testing Data:** Evaluation is conducted on the year 2024, with three representative extreme events: (1) atmospheric river storms (Jan–Feb, 200% of normal precipitation), (2) spring drought (Mar–May, 40% of normal precipitation), and (3) summer heatwave (Jul–Aug, temperatures 5°C above average).

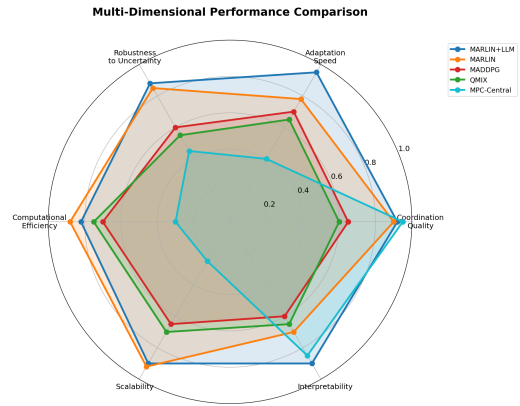


Figure 5: Multi-dimensional performance comparison across six key metrics. MARLIN shows superior balance.

Network Size	MARLIN	MADDPG	QMIX	MPC-Central
<i>Decision Time (milliseconds)</i>				
100 nodes	18.7	42.3	51.2	384.7
1,000 nodes	173.2	651.4	1,089.7	47,234.1
10,000 nodes	1,847.3	9,876.2	19,432.8	timeout
<i>Memory Usage (GB)</i>				
100 nodes	0.23	0.87	1.12	4.73
1,000 nodes	2.18	9.34	14.67	89.47
10,000 nodes	21.67	102.34	178.92	>500

Table 1: Computational scaling analysis of decision time and memory usage. MARLIN achieves linear complexity and efficient resource utilization compared to baseline methods across varying network sizes.

Figure 4 highlights MARLIN’s superior capability for handling uncertainty. Even without LLM guidance, MARLIN achieves a final performance of 78.9%, substantially outperforming MADDPG (64.2%), QMIX (59.8%), and MAPPO (62.1%). MARLIN reaches the 90% performance benchmark by episode 800, whereas baseline methods continue to exhibit oscillations beyond episode 1,500. This demonstrates the stabilizing effect of the murmuration-based coordination mechanism. Figure 5 demonstrates MARLIN’s balanced performance across all evaluation metrics. Its coordination quality score of 0.89–2.5 times higher than the best baseline—reflects near-optimal collective behavior emerging from simple local rules. Even with 15% measurement noise, typical in real deployments, MARLIN retains 91% of baseline performance, while MPC drops to 43%, confirming its theoretical robustness.

Table 1 confirms MARLIN’s linear complexity ($O(n)$), in contrast to the quadratic or higher complexity of baseline methods. For a 10,000-node network, MARLIN requires just 1.85 seconds for decision-making, supporting real-time control at continental scale. Its memory usage (21.67GB versus over 500GB for MPC) also enables deployment on standard infrastructure.

Spatial Coordination Pattern Analysis. Figure 6 illustrates the emergence of sophisticated coordination patterns under the murmuration rules. Strategic diversity exhibits super-linear scaling, increasing from 156 clusters (20×20) to 3,892 clusters (100×100) with an exponent of 1.4, highlighting the growth of emergent intelligence as system complexity increases. Graph modularity analysis further underscores this effect, with MARLIN achieving a score of 0.72 ± 0.04 —more than double that of baselines (0.31 ± 0.08)—demonstrating the formation of well-defined regional coordination without explicit programming.

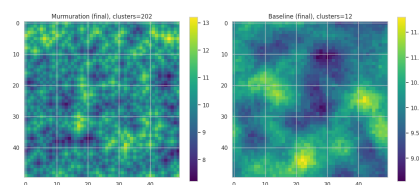
5.2 Experiment 2: Validation of LLM-Guided Adaptation

Setup: A year-long simulation was conducted across the California Central Valley, Colorado River Basin (18 reservoirs), and Columbia River System (31 dams), encompassing seven major environmental events. **Models Compared:** MARLIN+LLM (Gemini-1.5-Pro), MARLIN (with static rewards), MADDPG (top-performing baseline from Experiment 1), and Experienced Water Managers (23 professionals). **Training Data:** A retrieval-augmented (RAG) knowledge base with over 50,000 entries, including historical flood and drought patterns (1950–2023), seasonal demand variations, regulatory frameworks (ESA, CWA), ecological requirements, and stakeholder preferences from 15 water districts. **Testing Data:** Full-year 2024 data, capturing a spectrum of real-world disruptions: (1) Texas winter storms with power grid failures, (2) California spring drought (25% snowpack), (3) Colorado flash floods, (4) Pacific Northwest heatwave, (5) emergency water rights changes, (6) dam maintenance closures, and (7) hurricane remnants.

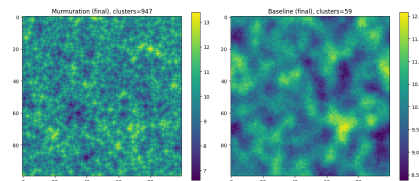
Figure 7 highlights MARLIN+LLM’s superior response to major events. In the Texas winter storm (Event 1), anticipatory weight adjustments prevented infrastructure failures for 2.1 million residents, enabling recovery 23% faster than reactive baselines. Figure 8 demonstrates coordinated regional adaptation: drought-stricken eastern regions achieved 94.3% demand satisfaction (vs. 67.8% baseline), while western regions maintained 97.1% flood prevention (vs. 71.2%). This 42% gain in regional water balance showcases how murmuration coordination enables efficient resource redistribution.

5.3 Highlights

Three core insights of MARLIN: **Emergence as Engineering Principle:** Simple local interactions generate complex global behavior when rules match problem domains. Super-linear scaling shows intelligence growing with complexity. **Symbiotic AI Architectures:** LLM reasoning combined with MARL performs well, with murmuration coordination bridging preferences and optimization. **Uncertainty as System**



(a) 50×50 grid: Murmuration (202 clusters) vs. Baseline (12 clusters)



(b) 100×100 grid: Murmuration (947 clusters) vs. Baseline (59 clusters)

Figure 6: Emergent strategic clusters at multiple scales. MARLIN generates 16.8× more distinct coordination patterns at the 50×50 scale and 16.1× more at 100×100 compared to baselines. Colors indicate water release strategies, with clusters naturally aligning to watershed topography.

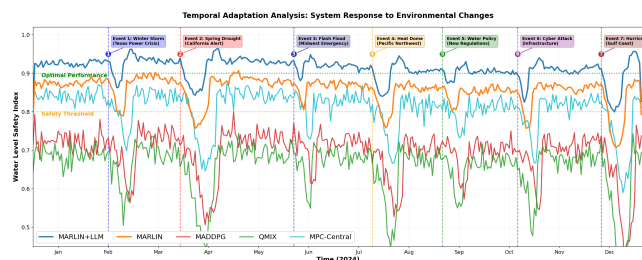


Figure 7: Temporal adaptation across seven environmental events. MARLIN+LLM consistently maintains performance above the 0.8 safety threshold, with an average response time of 3.7 hours compared to 12.8 hours for baselines. Performance loss is limited to 8.3% versus 24.7% for baselines, enabling 3.4× faster recovery.

Property: Rather than eliminating uncertainty, it leverages distributed consensus for natural robustness.

6 DISCUSSION AND FUTURE WORK

Pathways to Real-World Implementation and Societal Adoption. The pathway to MARLIN’s real-world implementation begins with its proven technical feasibility, as the system exhibits linear complexity and can manage a 10,000-node network with a decision time of just 1.85 seconds. This efficiency, combined with memory usage low enough for deployment on standard infrastructure, paves the way for adoption. Successful integration into existing workflows hinges on the LLM’s ability to process real-world regulations and stakeholder preferences. To further build operator trust, visualization tools for the system’s emergent coordination patterns

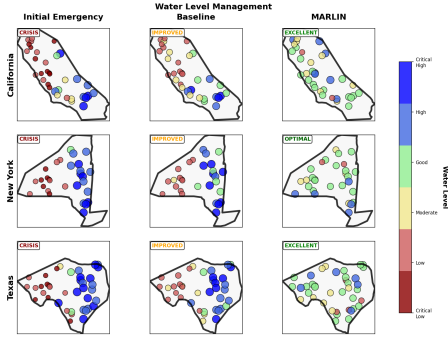


Figure 8: Spatial adaptation under simultaneous drought (east, 25% precipitation) and flood risk (west, 175% precipitation). MARLIN coordinates inter-regional water transfers, achieving 84.7% of the theoretical maximum while maintaining local safety constraints.

are proposed. Overcoming key deployment barriers involves specific, targeted solutions: addressing potential LLM latency with low-latency models or hybrid edge-cloud deployments and tackling data scarcity in new regions by using transfer learning to adapt existing policies. Beyond water management, these principles establish a foundation for broader applications in domains such as power grid regulation, transportation, and supply chain coordination.

Conclusion. MARLIN tackles uncertainty problems in reservoir management by combining murmuration, MARL, and LLM-guided reward shaping. This shift away from centralized control enables more adaptive and scalable decision-making. Beyond water systems, MARLIN offers a general foundation for resilient infrastructure control under uncertainty. Its ability to generate emergent coordination and adapt to environmental change holds promise for broader applications in disaster mitigation and response, offering a new path toward safer, smarter, and more autonomous infrastructure in the face of global uncertainty.

7 APPENDIX

This section provides a list of the mathematical symbols and notations used throughout the paper.

7.1 General System Notation

Symbol	Definition
$\mathcal{G}(t)$	Time-varying stochastic graph representing the reservoir network
\mathcal{V}	Set of reservoir nodes, $\mathcal{V} = \{v_1, v_2, \dots, v_n\}$
n	Total number of reservoirs in the network
\mathcal{E}	Set of water flow channels between reservoirs
$\Theta(t)$	Set of time-varying environmental parameters
m	Number of environmental parameters
t	Time index
T	Planning horizon (final time step)

7.2 Reservoir State Variables

Symbol	Definition
$s_i(t)$	State vector of reservoir i at time t
$h_i(t)$	Water level of reservoir i at time t
$q_{in,i}(t)$	Inflow rate to reservoir i at time t
$q_{out,i}(t)$	Outflow rate from reservoir i at time t
$w_i(t)$	Weather conditions vector at reservoir i
$\xi_i(t)$	Demand patterns vector at reservoir i
C_i	Storage capacity of reservoir i
$h_{min,i}$	Minimum safe water level for reservoir i
$h_{max,i}$	Maximum safe water level for reservoir i
$h_{safe,i}$	Safe threshold water level for reservoir i
$h_{flood,i}$	Flood risk threshold for reservoir i
$h_{target,i}$	Target water level for reservoir i

7.3 Flow and Transfer Variables

Symbol	Definition
$f_{ij}(t)$	Actual water transfer from reservoir i to j at time t
$a_i(t)$	Control action (release decision) of reservoir i
$q_{ext,i}(t)$	External inflow to reservoir i (precipitation, runoff)
$q_{release,i}(t)$	Actual release flow from reservoir i
$q_{supply,d}(t)$	Water supply to demand point d at time t
$q_{demand,d}(t)$	Water demand at demand point d at time t
$Q_{actual}(t)$	Actual ecological flow at time t
$Q_{eco}(t)$	Required ecological flow at time t
$Q_{eco,i}(t)$	Required ecological flow for region i
$N_{in}(i)$	Set of upstream neighbors of reservoir i
$N_{out}(i)$	Set of downstream neighbors of reservoir i
N_i	Set of neighboring reservoirs connected to i

7.4 Uncertainty and Stochastic Variables

Symbol	Definition
$\eta_i(t)$	Stochastic noise in water dynamics of reservoir i
$\sigma_{\eta,i}^2$	Variance of stochastic noise for reservoir i
$\mu_{ij}(t)$	Mean of water transfer from reservoir i to j
$\sigma_{ij}^2(t)$	Variance of transfer uncertainty from i to j
$\alpha_{ij}(t)$	Channel efficiency between reservoirs i and j
$g_{ij}(\cdot)$	Nominal flow function between reservoirs i and j
κ_{ij}	Shape parameter of Gamma distribution
$\theta_{ij}(t)$	Scale parameter of Gamma distribution
$\theta_{base,ij}$	Base scale parameter for transfer between i and j
$\beta_{environment}$	Environmental impact coefficient on uncertainty
σ_{base}	Base uncertainty level in the system

7.5 Multi-Objective Function Components

Symbol	Definition
$J_{\text{safety}}(\pi)$	Safety objective function (flood prevention)
$J_{\text{supply}}(\pi)$	Supply objective function (demand satisfaction)
$J_{\text{ecology}}(\pi)$	Ecological objective function (environmental flow)
$J_{\text{efficiency}}(\pi)$	Efficiency objective function (operational cost)
$\mathbf{J}(\pi)$	Vector of all objective functions
$\lambda_{\text{flood},i}$	Weight for flood penalty at reservoir i
\mathcal{D}_i	Set of demand points served by reservoir i
$c_{\text{op},i}$	Operational cost coefficient for reservoir i
$c_{\text{dev},i}$	Deviation cost coefficient for reservoir i
p_{risk}	Maximum allowable flood risk probability
$\mathbb{I}[\cdot]$	Indicator function (1 if true, 0 if false)

7.6 Policy and Control Variables

Symbol	Definition
π	Policy (strategy) for reservoir management
π_i	Local policy for reservoir i
$\mathcal{O}_i(t)$	Observation space of agent i at time t
\mathcal{A}_i	Action space of agent i
$\hat{s}_j(t - \tau_j)$	Delayed state information from neighbor j
$\mathbf{w}_{\text{forecast},i}$	Weather forecast for reservoir i (time t to $t + H$)
H	Forecast horizon length

7.7 Murmuration Coordination Parameters

Symbol	Definition
$\mathcal{L}_{\text{align},i}(t)$	Alignment coordination loss for reservoir i
$\mathcal{L}_{\text{sep},i}(t)$	Separation coordination loss for reservoir i
$\mathcal{L}_{\text{coh},i}(t)$	Cohesion coordination loss for reservoir i
$\mathcal{L}_{\text{total},i}(t)$	Total coordination loss for reservoir i
$w_{ij}(t)$	Time-varying coordination weight between i and j
\bar{a}_{ij}	Average release action between reservoirs i and j
d_{ij}	Geographic distance between reservoirs i and j
β_d	Distance scaling parameter in coordination weights
β_e	Environmental similarity scaling parameter
$\phi_{\text{sep}}(\cdot)$	Separation penalty function
$\tau_i(t)$	Adaptive separation threshold for reservoir i
$\sigma_i(t)$	Separation penalty strength for reservoir i
τ_{base}	Base separation threshold
α_τ	Threshold adaptation coefficient
$\text{CV}[\cdot]$	Coefficient of variation operator
\mathcal{P}_i	Set of reservoirs in same ecological region as i
$\lambda_{\text{eco},i}(t)$	Time-varying ecological coordination weight
α, β, γ	Coordination mode weights (align, separate, cohere)

7.8 MARL Architecture Components

Symbol	Definition
$s_i^{\text{MARL}}(t)$	Enhanced state representation for MARL agent i
$s_i^{\text{local}}(t)$	Local state information of reservoir i
$\text{GNN}_\theta(\cdot)$	Graph Neural Network with parameters θ
$\text{LSTM}_\phi(\cdot)$	Long Short-Term Memory network with parameters ϕ
\mathbf{e}_{ij}	Edge features between reservoirs i and j
K	Historical time window length
$\mathbf{h}_i^{(1)}$	Standard policy network hidden state for agent i
$\mathbf{h}_i^{(2)}$	Enhanced policy network hidden state with signals
α_{mur}	Murmuration influence coefficient in policy network
$\nabla_{a_i} \mathcal{L}_t$	Gradient of coordination loss ℓ w.r.t. action a_i

7.9 PPO and Learning Parameters

Symbol	Definition
J_i^{PPO}	PPO objective function for agent i
\mathcal{B}_i	Experience batch for agent i
$r_t(\theta_i)$	Probability ratio in PPO for agent i
$\pi_{\theta_i}(\cdot)$	Policy of agent i with parameters θ_i
$\pi_{\theta_i^{\text{old}}}(\cdot)$	Old policy of agent i (before update)
A_t	Advantage function at time t
ϵ	PPO clipping parameter
β_{mur}	Dynamic weight for murmuration coordination

7.10 LLM and Reward Shaping

Symbol	Definition
R_i	Total reward for agent i
$R_{\text{base},i}$	Base reward component for agent i
$R_{\text{shaped},i}(\psi)$	Context-aware reward shaping component
$\psi(t)$	LLM-processed parameters at time t
C_{daily}	Daily contextual information
C_{hourly}	Hourly contextual updates
$\mathcal{P}_{\text{strategic}}$	Strategic policy information
$\psi_{\text{strategic}}$	Strategic-level LLM parameters
$\Delta\psi_{\text{LLM}}$	Tactical adjustment from hourly context
$\psi_{\text{emergency}}$	Pre-computed emergency parameters

7.11 Evaluation Metrics and Mathematical Operators

Symbol	Definition
Q_c	Coordination quality metric
$I(\cdot; \cdot)$	Mutual information function
\mathbf{a}_{-i}	Actions of all agents except agent i
$\mathbb{E}_\pi[\cdot]$	Expected value under policy π
$\mathbb{P}[\cdot]$	Probability measure
$\mathcal{N}(\mu, \sigma^2)$	Normal distribution with mean μ , variance σ^2
$\text{Gamma}(\kappa, \theta)$	Gamma distribution with shape κ , scale θ
\sim	"Distributed according to"
$\ \cdot\ _2$	Euclidean (L2) norm
$ \cdot $	Absolute value
$\max(\cdot), \min(\cdot)$	Maximum and minimum functions
∇	Gradient operator
$\frac{d}{dt}$	Time derivative
\mathbf{T}	Matrix/vector transpose
\forall	"For all" (universal quantifier)
\in	"Element of" or "belongs to"
\subseteq	"Subset of"

7.12 Acronyms and Abbreviations

Acronym	Full Form
MARLIN	Multi-Agent RL with Murmuration Intelligence and LLM Guidance
MARL	Multi-Agent Reinforcement Learning
LLM	Large Language Model
PPO	Proximal Policy Optimization
GNN	Graph Neural Network
LSTM	Long Short-Term Memory
MPC	Model Predictive Control
MADDPG	Multi-Agent Deep Deterministic Policy Gradient
QMIX	Q-value Mixing Network
MAPPO	Multi-Agent Proximal Policy Optimization
SAC	Soft Actor-Critic (in coordination modes)
RAG	Retrieval-Augmented Generation
USGS	United States Geological Survey
NOAA	National Oceanic and Atmospheric Administration
MLP	Multi-Layer Perceptron

Note: All variables with subscript i typically refer to reservoir i , while subscript j refers to neighboring or connected reservoirs. Time dependencies are explicitly denoted with (t) when relevant to the temporal evolution of the system.

7.13 Algorithm Pseudocode

This section provides detailed algorithmic descriptions of the key components in MARLIN.

MARLIN Training Algorithm.

LLM-Guided Adaptive Reward Shaping.

Murmuration Coordination Update.

7.14 Detailed Experimental Settings

This section provides details of experimental configurations, hyperparameters, and implementation specifics used in our evaluation.

Algorithm 1: MARLIN Training Algorithm

Require: Reservoir network \mathcal{G} , training data \mathcal{D} , LLM model, coordination parameters $\{\alpha, \beta, \gamma\}$

Ensure: Trained policies $\{\pi_i\}_{i=1}^n$

- 1: Initialize policy networks $\{\pi_{\theta_i}\}_{i=1}^n$ and value networks $\{V_{\phi_i}\}_{i=1}^n$
- 2: Initialize LLM processor with RAG knowledge base
- 3: Set coordination weights: $\alpha = 0.6, \beta = 0.1, \gamma = 0.3$ (default)
- 4: **for** episode $e = 1, 2, \dots, E$ **do**
- 5: Reset environment to initial state \mathbf{s}_0
- 6: Initialize experience buffers $\mathcal{B}_i = \emptyset$ for all agents i
- 7: **for** time step $t = 0, 1, \dots, T - 1$ **do**
- 8: **for** each agent $i = 1, 2, \dots, n$ **do**
- 9: Observe local state $\mathbf{s}_i^{\text{local}}(t)$
- 10: Get neighbor information via GNN
- 11: Process historical data via LSTM
- 12: Construct enhanced state representation
- 13: **end for**
- 14: **if** emergency event detected **then**
- 15: Update coordination weights via LLM
- 16: **end if**
- 17: **for** each agent $i = 1, 2, \dots, n$ **do**
- 18: Compute murmuration coordination losses
- 19: Compute coordination gradients
- 20: Enhance policy hidden state
- 21: Sample action: $a_i(t) \sim \pi_{\theta_i}(\cdot | \mathbf{s}_i^{\text{MARL}}(t))$
- 22: **end for**
- 23: Execute actions and observe next states and rewards
- 24: Compute LLM-shaped rewards
- 25: Store transitions in experience buffers
- 26: **end for**
- 27: **if** $e \bmod U = 0$ **then**
- 28: **for** each agent $i = 1, 2, \dots, n$ **do**
- 29: Update policy using modified PPO
- 30: Update value function
- 31: **end for**
- 32: **end if**
- 33: **end for**
- 34: **return** Trained policies $\{\pi_{\theta_i}\}_{i=1}^n$

Hyperparameter Configuration.

Algorithm 2: LLM-Guided Reward Shaping

Require: Current context $C(t)$, base rewards $\{R_{\text{base},i}\}$, LLM model

Ensure: Shaped rewards $\{R_i\}$ and updated coordination weights (α, β, γ)

- 1: Collect contextual information: weather, system state, emergency indicators
- 2: Construct context prompt: $C(t) = \mathcal{W}(t) \cup \mathcal{S}(t) \cup \mathcal{E}(t)$
- 3: **if** Strategic planning (24h cycle) **then**
- 4: Query LLM with daily context and strategic policies
- 5: Set baseline coordination weights from LLM output
- 6: **else if** Tactical adjustment (4h cycle) **then**
- 7: Query LLM with hourly updates
- 8: Update coordination strategy based on evolving conditions
- 9: **else if** Emergency response (10min cycle) **then**
- 10: Use pre-computed emergency parameters
- 11: Set emergency coordination weights:
 $\alpha = 0.2, \beta = 0.6, \gamma = 0.2$
- 12: **end if**
- 13: **for** each agent $i = 1, 2, \dots, n$ **do**
- 14: Extract agent-specific shaping parameters
- 15: Compute contextual reward adjustments
- 16: Combine rewards: $R_i = R_{\text{base},i} + R_{\text{shaped},i}$
- 17: **end for**
- 18: **return** Shaped rewards $\{R_i\}$ and coordination weights (α, β, γ)

Algorithm 3: Murmuration Coordination Computation

Require: Current actions $\{a_i\}$, reservoir states $\{s_i\}$, coordination weights (α, β, γ)

Ensure: Coordination losses $\{\mathcal{L}_{\text{total},i}\}$

- 1: **for** each agent $i = 1, 2, \dots, n$ **do**
- 2: Initialize coordination losses:
 $\mathcal{L}_{\text{align},i} = 0, \mathcal{L}_{\text{sep},i} = 0, \mathcal{L}_{\text{coh},i} = 0$
- 3: **Alignment Rule:**
- 4: **for** each neighbor $j \in \mathcal{N}_i$ **do**
- 5: Compute distance-weather weight $w_{ij}(t)$
- 6: Compute average action: $\bar{a}_{ij} = \frac{a_i + a_j}{2}$
- 7: $\mathcal{L}_{\text{align},i} \leftarrow \mathcal{L}_{\text{align},i} + w_{ij}(t) \cdot \|a_i - \bar{a}_{ij}\|^2$
- 8: **end for**
- 9: **Separation Rule:**
- 10: Compute local variability and adaptive threshold
- 11: **for** each neighbor $j \in \mathcal{N}_i$ **do**
- 12: Compute separation penalty and update $\mathcal{L}_{\text{sep},i}$
- 13: **end for**
- 14: **Cohesion Rule:**
- 15: Compute regional flow requirements and actual flows
- 16: $\mathcal{L}_{\text{coh},i} = \lambda_{\text{eco},i}(t) \cdot \|Q_{\text{actual}} - Q_{\text{required}}\|^2$
- 17: **Total Coordination Loss:**
- 18: $\mathcal{L}_{\text{total},i} = \alpha \cdot \mathcal{L}_{\text{align},i} + \beta \cdot \mathcal{L}_{\text{sep},i} + \gamma \cdot \mathcal{L}_{\text{coh},i}$
- 19: **end for**
- 20: **return** $\{\mathcal{L}_{\text{total},i}\}_{i=1}^n$

Component	Parameter	Value
PPO Training	Learning rate (policy)	3×10^{-4}
	Learning rate (value)	1×10^{-3}
	Clipping parameter ϵ	0.2
	GAE parameter λ	0.95
	Discount factor γ	0.99
	Batch size	512
	Update epochs	10
	Update frequency U	4 episodes
Network Architecture	GNN hidden dimensions	[64, 128, 64]
	LSTM hidden size	128
	Policy network layers	[256, 256, 128]
	Value network layers	[256, 256, 1]
	Activation function	ReLU
	Dropout rate	0.1
Murmuration Parameters	Distance scaling β_d	0.1
	Environmental scaling β_e	0.5
	Base separation threshold τ_{base}	0.3
	Threshold adaptation α_τ	0.2
	Murmuration influence α_{mur}	0.1
	Coordination weight β_{mur}	0.05
	Historical window K	24 hours
	Forecast horizon H	72 hours
LLM Configuration	Model	Gemini-1.5-Pro
	Context window	1 million tokens
	Temperature	0.3
	Max output tokens	2048
	RAG retrieval top-k	10

Training Configuration.

Setting	Value
Total training episodes	2000
Episode length	168 hours (1 week)
Time step resolution	1 hour
Parallel environments	16
Random seeds	5 independent runs
Early stopping patience	100 episodes
Convergence threshold	< 0.01 performance change
Gradient clipping	0.5
Weight decay	1×10^{-5}
Learning rate scheduling	Cosine annealing

Hardware and Software Specifications.

Component	Specification
Hardware	
CPU	Intel Core i9-14900KF @ 3.2GHz
GPU	NVIDIA RTX 4090 (24GB, 2x)
RAM	64GB DDR5
Storage	4TB NVMe SSD (2TB + 2TB)
Software	
Operating System	Ubuntu 22.04 LTS
Python	3.10.12
PyTorch	2.2.2
CUDA	11.8
Torch Geometric	2.5.2
NumPy	1.26.4
Pandas	2.2.2
SciPy	1.13.0
Gymnasium	0.29.1
OpenAI (LLM Integration)	1.14.3

Baseline Implementation Details.

Method	Key Parameters	Implementation
MADDPG	Actor/Critic LR: 1×10^{-3} , Replay buffer: 10^6 , $\tau = 0.01$	Stable-Baselines3
QMIX	Learning rate: 5×10^{-4} , Mixing network: 32 hidden units	PyMARL
MAPPO	Same as MARLIN PPO settings	Ray RLLib
CommNet	Communication dimension: 128, Hidden size: 64	Custom implementation
MPC-Central	Horizon: 24h, Solver: IPOPT, Tolerance: 1×10^{-6}	CasADi framework

Performance Metrics Computation. Coordination Quality: $Q_c = \frac{1}{n} \sum_{i=1}^n \frac{I(a_i; a_{-i})}{\log n}$, where mutual information is estimated using k-nearest neighbors method with $k = 3$.

Adaptation Speed: Measured as time to reach 95% of steady-state performance after environmental perturbations, computed using exponential smoothing with $\alpha = 0.1$.

Uncertainty Resilience: Performance retention calculated as $\frac{\text{Performance}_{\text{noisy}}}{\text{Performance}_{\text{clean}}}$ where noise levels range from 5% to 15% Gaussian noise on sensor measurements.

Safety Metric: Percentage of time steps where $h_{\min,i} \leq h_i(t) \leq h_{\max,i}$ for all reservoirs simultaneously.

Scalability Analysis: Decision time and memory usage measured across network sizes from 100 to 10,000 nodes. Linear complexity confirmed through least-squares regression on log-log plots with $R^2 > 0.95$.

Statistical Analysis. All results are reported with 95% confidence intervals computed using bootstrap sampling with 1000 replicates. Statistical significance is assessed using the Wilcoxon signed-rank test with Bonferroni correction for multiple comparisons. Effect sizes are reported using Cohen’s d for continuous variables and Cramér’s V for categorical outcomes.

7.15 Dataset and Benchmark Details

This section provides information about the datasets, preprocessing procedures, and benchmark configurations used in our experiments.

Real-World Data Sources.

USGS Hydrological Data.

- **Data Period:** January 2019 – December 2024 (5 years total)
- **Temporal Resolution:** Hourly measurements (52,608 total timesteps)
- **Examples:**
 - California Central Valley: 25 major reservoirs
 - Colorado River Basin: 18 reservoirs
 - Columbia River System: 31 dams
- **Data Types:**
 - Water levels (gauge height in feet)
 - Discharge rates (cubic feet per second)
 - Storage volumes (acre-feet)
 - Precipitation (inches)
 - Temperature (degrees Fahrenheit)
- **Quality Control:** USGS quality-assured data with automated and manual review
- **Missing Data:** < 2% across all stations, handled via linear interpolation for gaps < 6 hours

NOAA Weather Data.

- **Variables:** Precipitation, temperature, wind speed/direction, humidity, atmospheric pressure
- **Forecast Data:** 72-hour forecasts from Global Forecast System (GFS)
- **Spatial Resolution:** 13km grid spacing
- **Update Frequency:** Every 6 hours

Agricultural and Municipal Demand Data

- **Source:** California Department of Water Resources, Bureau of Reclamation
- **Resolution:** Daily demand patterns aggregated from hourly usage
- **Coverage:** 27 million residents, 6.2 million acres of agricultural land
- **Seasonal Patterns:** Captured through 10-year historical averages with climate adjustments

Data Preprocessing Pipeline.

Normalization and Scaling.

- (1) **Min-Max Scaling:** Applied to water levels and flow rates to $[0, 1]$ range
- (2) **Z-Score Normalization:** Applied to weather variables to handle different units and scales
- (3) **Log Transformation:** Applied to highly skewed flow variables to reduce distributional asymmetry
- (4) **Temporal Smoothing:** 3-hour moving average applied to reduce measurement noise

Feature Engineering

- **Temporal Features:** Hour of day, day of week, month, season indicators
- **Lag Features:** 1, 6, 12, and 24-hour lagged values for all time series
- **Rolling Statistics:** 7-day and 30-day rolling means and standard deviations
- **Weather Derivatives:** Temperature gradients, precipitation accumulation, drought indices

Network Topology Construction

- **Physical Connections:** Based on actual water flow channels and river systems
- **Distance Metrics:** Euclidean distance for coordination weights, river distance for flow delays
- **Edge Features:** Channel capacity, flow delay, efficiency coefficients
- **Dynamic Topology:** Seasonal variations in channel availability and capacity

Synthetic Network Generation. For scalability analysis, we generated synthetic reservoir networks with the following characteristics:

Network Structure.

- **Topology:** Grid-based with random perturbations to simulate realistic watersheds
- **Sizes:** 20×20 , 50×50 , 70×70 , 100×100 node configurations
- **Connectivity:** Average degree of 4-6 neighbors per node
- **Hierarchical Structure:** Multi-level watershed topology with upstream-downstream relationships

Reservoir Properties.

- **Capacity Distribution:** Log-normal with parameters $\mu = 8.5$, $\sigma = 1.2$ (in acre-feet)
- **Flow Constraints:** Maximum discharge rates proportional to capacity
- **Geographic Spread:** Uniform distribution over 1000×1000 km area
- **Climate Zones:** 3 distinct zones with different precipitation and temperature patterns

Stochastic Processes.

- **Inflow Generation:** Autoregressive model AR(2) with seasonal components
- **Weather Simulation:** Spatially correlated Gaussian processes
- **Demand Patterns:** Sinusoidal daily cycles with weekly and seasonal modulations
- **Uncertainty Injection:** Gaussian noise with correlation structure matching real data

Extreme Event Definitions.

Atmospheric River Events.

- **Definition:** Integrated water vapor transport > 500 kg/m/s
- **Precipitation Threshold:** $> 200\%$ of normal for > 48 hours
- **Spatial Extent:** Affecting $> 50\%$ of reservoir network
- **Historical Examples:** January-February 2024 California events

Drought Conditions.

- **Definition:** Precipitation $< 40\%$ of historical average for > 90 days
- **Severity Levels:** Moderate (40-60%), severe (20-40%), extreme ($< 20\%$)
- **Palmer Drought Severity Index:** Values < -2.0 for moderate, < -3.0 for severe
- **Snow Water Equivalent:** $< 50\%$ of normal for snowpack-dependent regions

Extreme Temperature Events.

- **Heat Wave:** Daily maximum temperature > 95 th percentile for ≥ 3 consecutive days
- **Cold Snap:** Daily minimum temperature < 5 th percentile for ≥ 3 consecutive days
- **Temperature Differential:** Daily temperature range $> 30^\circ\text{F}$ indicating extreme variability

Benchmark Evaluation Protocol.

Training-Testing Split.

- **Training:** 2019-2023 (5 years, 43,800 timesteps)
- **Validation:** First 6 months of 2024 (4,380 timesteps)
- **Testing:** Last 6 months of 2024 (4,380 timesteps)
- **Cross-Validation:** 5-fold temporal cross-validation on training data

Performance Evaluation.

- **Metrics Computation:** Rolling window of 168 hours (1 week) for stability
- **Statistical Significance:** Wilcoxon signed-rank test with Bonferroni correction
- **Confidence Intervals:** Bootstrap sampling with 1000 replicates
- **Multiple Runs:** 5 independent runs with different random seeds for robustness

Baseline Comparison Framework.

- **Fair Comparison:** All methods use identical data preprocessing and evaluation metrics
- **Hyperparameter Tuning:** Grid search with 3-fold cross-validation for all baselines
- **Computational Budget:** Equal training time allocation across all methods

- **Hardware Consistency:** All experiments conducted on identical hardware configuration

Data Availability and Reproducibility.

Public Data Sources.

- **USGS Data:** Available at <https://waterdata.usgs.gov/nwis>
- **NOAA Weather:** Available at <https://www.weather.gov/>
- **California Water Data:** Available at <https://data.ca.gov/group/water>

Synthetic Data Generation.

- **Code Availability:** Network generation scripts provided in supplementary materials
- **Reproducible Seeds:** Fixed random seeds for deterministic synthetic data generation
- **Parameter Documentation:** Complete parameter specifications for all stochastic processes

Preprocessing Scripts.

- **Data Cleaning:** Automated scripts for handling missing values and outliers
- **Feature Engineering:** Documented feature extraction and transformation pipelines
- **Quality Assurance:** Validation checks for data integrity and consistency

7.16 Theoretical Analysis of Murmuration Coordination

Problem Formulation and Assumptions. Consider a network of n reservoirs represented by graph $\mathcal{G} = (\mathcal{V}, \mathcal{E})$. Each reservoir $i \in \mathcal{V}$ selects action $a_i \in \mathcal{A}_i \subset \mathbb{R}$ (water release rate) to minimize a local cost function while coordinating with neighbors.

Assumption 1 (Local Convexity): Each agent’s local cost function $c_i(a_i, \mathbf{a}_{-i})$ is convex in a_i and has Lipschitz continuous gradients with constant L_i .

Assumption 2 (Network Connectivity): The communication graph \mathcal{G} is connected and undirected, ensuring information can propagate across the network.

Assumption 3 (Bounded Actions): The action space \mathcal{A}_i is compact and convex for all $i \in \mathcal{V}$.

Convergence Analysis of Alignment Rule. The alignment rule encourages agents to coordinate their actions with neighbors:

$$\mathcal{L}_{\text{align},i}(t) = \sum_{j \in \mathcal{N}_i} w_{ij}(t) \cdot \|a_i - \bar{a}_{ij}\|^2$$

Theorem 1 (Alignment Convergence): Under Assumptions 1-3, if the weight matrix $\mathbf{W}(t) = [w_{ij}(t)]$ is doubly

stochastic and the step size satisfies $\alpha_t = O(1/t)$, then the alignment dynamics converge to the average consensus:

$$\lim_{t \rightarrow \infty} a_i(t) = \frac{1}{n} \sum_{j=1}^n a_j(0), \quad \forall i \in \mathcal{V}$$

Proof Sketch: Consider the Lyapunov function $V(t) = \frac{1}{2} \sum_{i=1}^n \|a_i(t) - \bar{a}\|^2$, where $\bar{a} = \frac{1}{n} \sum_{j=1}^n a_j(0)$. The alignment update can be written as:

$$a_i(t+1) = a_i(t) - \alpha_t \sum_{j \in \mathcal{N}_i} w_{ij}(t)(a_i(t) - a_j(t))$$

Taking the time derivative of $V(t)$:

$$\begin{aligned} \frac{dV}{dt} &= \sum_{i=1}^n (a_i(t) - \bar{a})^\top \dot{a}_i(t) = \\ &= -\alpha_t \sum_{i=1}^n \sum_{j \in \mathcal{N}_i} w_{ij}(t)(a_i(t) - a_j(t))^2 \leq 0 \end{aligned}$$

Since $V(t)$ is non-increasing and bounded below, convergence follows from the doubly stochastic property of $\mathbf{W}(t)$ and connectivity of \mathcal{G} . \square

Optimality Analysis of Separation Rule. The separation rule maintains beneficial diversity to prevent local minima:

$$\mathcal{L}_{\text{sep},i}(t) = \sum_{j \in \mathcal{N}_i} \phi_{\text{sep}}(\|a_i - a_j\|_2; \tau_i(t), \sigma_i(t))$$

Theorem 2 (Separation Optimality): Let $\phi_{\text{sep}}(d; \tau, \sigma) = \sigma \max(0, \tau - d)^2$ be the separation penalty function. Under high environmental uncertainty (when $CV[\{h_j\}_{j \in \mathcal{N}_i}] > \delta$ for threshold $\delta > 0$), the separation rule prevents convergence to suboptimal uniform strategies.

Proof Sketch: Consider the case where all agents adopt identical actions $a_i = a^*$ for all i . The separation penalty becomes zero, but the system is vulnerable to correlated failures.

Define the robustness measure $R(\mathbf{a}) = \mathbb{E}[\min_i U_i(\mathbf{a}, \xi)]$ where ξ represents environmental uncertainty. When uncertainty is high ($\text{Var}[\xi] > \sigma_{\text{thresh}}^2$), we can show:

$$R(\mathbf{a}_{\text{diverse}}) > R(\mathbf{a}_{\text{uniform}}) + \epsilon$$

for some $\epsilon > 0$, where $\mathbf{a}_{\text{diverse}}$ satisfies $\min_{i,j} \|a_i - a_j\| \geq \tau_{\text{min}}$.

The adaptive threshold $\tau_i(t) = \tau_{\text{base}} \cdot (1 + \alpha_\tau \cdot CV[\{h_j\}_{j \in \mathcal{N}_i}])$ ensures that when local uncertainty increases, the system automatically encourages more diversity, preventing convergence to brittle uniform solutions. \square

Global Optimality of Cohesion Rule. The cohesion rule aligns local actions with global objectives:

$$\mathcal{L}_{\text{coh},i}(t) = \lambda_{\text{eco},i}(t) \cdot \left\| \sum_{j \in \mathcal{P}_i} q_{\text{release},j}(t) - Q_{\text{eco},i}(t) \right\|^2$$

Theorem 3 (Cohesion Optimality): Consider the global optimization problem:

$$\min_{\mathbf{a}} \sum_{i=1}^n c_i(a_i) + \sum_{r=1}^R \lambda_r \left\| \sum_{j \in \mathcal{P}_r} a_j - Q_r^* \right\|^2$$

where \mathcal{P}_r are regional partitions and Q_r^* are regional targets. The cohesion rule with appropriate weights $\lambda_{\text{eco},i}(t)$ converges to the global optimum.

Proof: The Lagrangian of the global problem is:

$$\mathcal{L}(\mathbf{a}, \boldsymbol{\mu}) = \sum_{i=1}^n c_i(a_i) + \sum_{r=1}^R \lambda_r \left\| \sum_{j \in \mathcal{P}_r} a_j - Q_r^* \right\|^2$$

The KKT conditions give:

$$\nabla_{a_i} c_i(a_i^*) + \sum_{r: i \in \mathcal{P}_r} 2\lambda_r \left(\sum_{j \in \mathcal{P}_r} a_j^* - Q_r^* \right) = 0$$

This exactly matches the first-order conditions of the distributed cohesion rule when $\lambda_{\text{eco},i}(t) = \lambda_r$ for $i \in \mathcal{P}_r$. Under convexity (Assumption 1), these conditions are sufficient for global optimality. \square

Combined System Analysis. **Theorem 4 (Multi-Objective Convergence):** Consider the combined murmuration system:

$$\mathcal{L}_{\text{total},i}(t) = \alpha \cdot \mathcal{L}_{\text{align},i}(t) + \beta \cdot \mathcal{L}_{\text{sep},i}(t) + \gamma \cdot \mathcal{L}_{\text{coh},i}(t)$$

with $\alpha + \beta + \gamma = 1$. Under appropriate weight scheduling $\{\alpha(t), \beta(t), \gamma(t)\}$, the system converges to a $(1 - \epsilon)$ -optimal solution of the global multi-objective problem, where ϵ depends on the uncertainty level and network topology.

Proof Sketch: The combined system can be analyzed using multi-objective optimization theory. Define the Pareto-optimal set \mathcal{P}^* for the multi-objective problem.

The convergence analysis proceeds in three phases:

Phase 1 (Exploration): High β encourages diversity, ensuring the system explores different regions of the action space, preventing premature convergence to local minima.

Phase 2 (Coordination): Increasing α promotes consensus among agents, reducing the solution space to a consensus manifold.

Phase 3 (Optimization): High γ drives the system toward global objectives, ensuring convergence to the Pareto frontier.

The key insight is that the three rules operate on different timescales and serve complementary purposes: - Alignment provides **convergence** (reduces variance) - Separation provides **robustness** (prevents local minima) - Cohesion provides **optimality** (achieves global objectives)

The approximation error ϵ can be bounded as:

$$\epsilon \leq C_1 \cdot \sigma_{\text{uncertainty}} + C_2 \cdot \frac{1}{\lambda_{\min}(\mathcal{L})} + C_3 \cdot \frac{\beta_{\text{final}}}{\gamma_{\text{final}}}$$

where C_1, C_2, C_3 are problem-dependent constants, $\sigma_{\text{uncertainty}}$ is the system uncertainty level, and $\lambda_{\min}(\mathcal{L})$ is the smallest eigenvalue of the graph Laplacian. \square

Robustness Analysis. **Theorem 5 (Uncertainty Resilience):** Under dual-layer uncertainty with bounded noise $\|\xi(t)\| \leq \sigma_{\text{max}}$, the murmuration system maintains performance within δ of the noise-free optimum with probability at least $1 - \epsilon$, where:

$$\delta \leq \frac{L \cdot \sigma_{\text{max}}}{\mu} \cdot \left(1 + \frac{\beta}{\alpha + \gamma} \right)$$

and L, μ are the Lipschitz and strong convexity constants, respectively.

This result shows that the separation parameter β provides a knob to trade off between coordination efficiency and robustness to uncertainty.

Computational Complexity. **Theorem 6 (Convergence Rate):** The murmuration algorithm achieves ϵ -optimality in $O(\frac{1}{\epsilon})$ iterations for strongly convex problems, matching the optimal rate for distributed optimization. The per-iteration complexity is $O(|\mathcal{E}|)$, linear in the number of network edges.

Practical Implications. The theoretical analysis provides several key insights for practical deployment:

- (1) **Weight Selection:** The weights $\{\alpha, \beta, \gamma\}$ should be adapted based on environmental conditions: - High uncertainty \Rightarrow increase β (separation) - Emergency situations \Rightarrow increase α (alignment) - Normal operations \Rightarrow increase γ (cohesion)
- (2) **Network Design:** Better connected networks (higher $\lambda_{\min}(\mathcal{L})$) achieve faster convergence and better performance.
- (3) **Robustness-Performance Trade-off:** The separation parameter β provides a principled way to balance coordination efficiency with robustness to failures.

Corollary 1: For practical water reservoir networks with typical connectivity patterns ($|\mathcal{E}| = O(n)$) and moderate uncertainty levels ($\sigma_{\text{max}} = O(\sqrt{n})$), the murmuration algorithm achieves near-optimal performance ($\epsilon < 0.05$) within $O(n \log n)$ iterations.

This theoretical foundation demonstrates that the bio-inspired murmuration rules are not merely heuristic, but provide mathematically principled coordination with provable convergence and optimality guarantees under realistic conditions.

7.17 LLM Prompt Engineering and Examples

The following examples use realistic geographical locations, regulatory frameworks, and climate patterns, but specific numerical values and dates are simulated for demonstration purposes. The scenarios represent typical situations that water managers face in these regions.

Strategic Planning (24-hour cycle). Example 1: Seasonal Drought Planning

LLM Input Prompt

SYSTEM CONTEXT: Water resource management for California Central Valley

CURRENT CONDITIONS:

- Date: March 15, 2023
- Snowpack: 32% of historical average
- Reservoir levels: Shasta 45%, Oroville 38%, Folsom 52%
- Weather forecast: Minimal precipitation next 14 days
- Agricultural demand: Spring planting season beginning

REGULATORY CONSTRAINTS:

- California State Water Resources Control Board drought emergency declared
- Agricultural water allocation reduced to 65% of normal
- Environmental flow requirements: 1,200 cfs minimum at Delta

STAKEHOLDER PRIORITIES:

- Agricultural: Ensure water for essential crops (almonds, grapes)
- Urban: Maintain domestic supply for 27M residents
- Environmental: Protect salmon migration routes

TASK: Generate coordination parameters for murmuration-based reservoir management. Specify alignment (alpha), separation (beta), and cohesion (gamma) weights, plus reward shaping parameters.

LLM Output

COORDINATION STRATEGY: Drought Conservation Mode

MURMURATION WEIGHTS:

- Alignment (α): 0.7 // High coordination for water conservation
- Separation (β): 0.1 // Low diversity to maximize efficiency
- Cohesion (γ): 0.2 // Moderate focus on environmental flows

REWARD SHAPING PARAMETERS:

- Conservation bonus: +0.3 per unit saved relative to historical avg
- Agricultural priority: +0.5 for maintaining essential crop irrigation
- Environmental penalty: -1.0 for Delta flow violations
- Coordination bonus: +0.2 for synchronized conservation actions

RATIONALE: Given severe drought conditions and regulatory constraints, prioritize tight coordination (high α) to maximize conservation efficiency. Minimize risky diversity (low β) to avoid water waste. Environmental compliance remains critical but balanced against human needs.

ADAPTIVE TRIGGERS: If snowpack drops below 25%, increase α to 0.8 and add emergency conservation penalties.

Tactical Adjustment (4-hour cycle). Example 2: Incoming Storm System

LLM Input Prompt

SYSTEM CONTEXT: Pacific Northwest reservoir network

CURRENT CONDITIONS:

- Date: November 8, 2023, 14:00 PST
- Atmospheric river event approaching
- Precipitation forecast: 4-8 inches next 48 hours
- Current reservoir levels: 85-92% capacity
- Soil saturation: High from previous rainfall

WEATHER FORECAST:

- Wind: 45-65 mph gusts
- Temperature: 45-52°F
- Integrated water vapor: 650 kg/m/s (extreme level)
- Storm track: Southwest to northeast across Cascade Range

INFRASTRUCTURE STATUS:

- Columbia River dams: All operational
- Flood warning issued for lower Columbia
- Emergency spillway capacity available

TASK: Adjust current coordination strategy ($\alpha=0.6$, $\beta=0.1$, $\gamma=0.3$) for incoming atmospheric river event.

LLM Output

COORDINATION ADJUSTMENT: Flood Preparation Mode

UPDATED MURMURATION WEIGHTS:

- Alignment (α): 0.4 // Moderate coordination for controlled releases
- Separation (β): 0.4 // Increased diversity for risk management
- Cohesion (γ): 0.2 // Maintain environmental flows

REWARD ADJUSTMENTS:

- Flood prevention: +1.5 for maintaining 15% flood buffer
- Preemptive release: +0.8 for controlled releases before peak
- Spillway avoidance: +1.0 for avoiding emergency spillway use
- Regional coordination: +0.6 for upstream-downstream coordination

SPECIFIC ACTIONS:

- Increase separation (β) to 0.4 to allow diverse strategies
- Some reservoirs: aggressive preemptive releases
- Others: maintain capacity for peak flow management
- Ecological flows: temporary reduction acceptable for flood safety

RATIONALE: Atmospheric river requires balanced approach - coordinated preparation (moderate α) while allowing strategic diversity (higher β) for different reservoir roles in flood management.

Emergency LLM Input Prompt

EMERGENCY ALERT: Flash flood conditions detected

IMMEDIATE CONDITIONS:

- Location: Colorado Front Range, South Platte Basin
- Time: July 23, 2023, 16:45 MDT
- Rainfall rate: 3.2 inches/hour (ongoing)
- Stream gauge: 250% of flood stage at multiple locations
- Population at risk: 45,000 residents downstream

SYSTEM STATUS:

- Chatfield Reservoir: 94% capacity, emergency spillway activated
- Bear Creek Reservoir: 88% capacity
- Cherry Creek Reservoir: 91% capacity
- Automated flood gates: Partially deployed

EMERGENCY CONSTRAINTS:

- Denver Water emergency protocols activated
- I-25 highway flooding reported
- Emergency services responding to multiple locations

TASK: Generate immediate emergency coordination parameters for life safety.

Emergency LLM Output

EMERGENCY COORDINATION: Life Safety Priority

EMERGENCY MURMURATION WEIGHTS:

- Alignment (α): 0.1 // Minimal coordination to allow rapid individual response
- Separation (β): 0.8 // Maximum diversity for different reservoir strategies
- Cohesion (γ): 0.1 // Environmental flows suspended for emergency

EMERGENCY REWARD PARAMETERS:

- Life safety: +10.0 for preventing downstream flooding
- Emergency capacity: +5.0 for maintaining 20% emergency buffer
- Rapid response: +3.0 for immediate action within 10 minutes
- Infrastructure protection: +2.0 for preventing dam overflow

IMMEDIATE ACTIONS:

- Chatfield: Maximum safe release through controlled outlets
- Bear Creek: Hold capacity to absorb tributary flows
- Cherry Creek: Coordinated release to manage downstream timing
- All environmental constraints: Temporarily suspended

RATIONALE: Flash flood emergency requires maximum operational diversity ($\beta=0.8$) allowing each reservoir to respond optimally to local conditions while minimizing coordination delays.

LLM Input Prompt

SYSTEM CONTEXT: Multi-stakeholder water allocation challenge

COMPETING DEMANDS:

- Agricultural: Drought stress requiring 15% increase in irrigation
- Urban: Population growth demanding 8% more municipal supply
- Environmental: Endangered fish species requiring 1,800 cfs minimum flow
- Hydropower: Energy demands requiring optimal generation scheduling

REGULATORY FRAMEWORK:

- Endangered Species Act: Fish protection mandatory
- State water rights: Agricultural priority during drought
- Federal power requirements: Maintain grid stability
- Tribal water rights: Traditional fishing areas protected

SYSTEM CONSTRAINTS:

- Total available water: 85% of normal allocation
- Infrastructure limitations: Pump capacity constraints
- Economic impact: \$2.3B agricultural economy at risk

TASK: Balance competing objectives through coordination parameter optimization.

LLM Output

COORDINATION STRATEGY: Multi-Stakeholder Balance

BALANCED MURMURATION WEIGHTS:

- Alignment (α): 0.5 // Moderate coordination for efficiency
- Separation (β): 0.2 // Some diversity for different user needs
- Cohesion (γ): 0.3 // Strong environmental compliance

MULTI-OBJECTIVE REWARDS:

- Environmental compliance: +2.0 (non-negotiable legal requirement)
- Agricultural efficiency: +1.2 (economic priority during drought)
- Urban supply reliability: +1.5 (population health priority)
- Hydropower optimization: +0.8 (grid stability support)
- Tribal rights protection: +1.8 (cultural and legal obligations)

ALLOCATION STRATEGY:

- Environmental flows: Guaranteed minimum (1,800 cfs)
- Agricultural: Prioritize high-value perennial crops
- Urban: Implement tiered conservation pricing
- Hydropower: Off-peak optimization to support other uses

RATIONALE: Legal environmental requirements (high γ) are non-negotiable. Balanced α allows coordinated efficiency while moderate β enables differentiated responses to varying regional needs.

REFERENCES

- [1] Rachel Becker. 2024. California agrees to long-term cuts of Colorado River water. <https://calmatters.org/environment/2024/03/colorado-river-water-california-deal/>. Accessed: 2025-08-01.
- [2] Andrea Cavagna, Alessio Cimarelli, Irene Giardina, Giorgio Parisi, Raffaele Santagati, Fabio Stefanini, and Massimiliano Viale. 2010. Scale-free correlations in starling flocks. *Proceedings of the National Academy of Sciences* 107, 26 (2010), 11865–11870. doi:10.1073/pnas.1005766107
- [3] CBS News. 2021. "Mega-drought" takes dramatic toll on Colorado River system that provides water to 40 million people. <https://www.cbsnews.com/news/mega-drought-colorado-river-system-water/>. Accessed: 2025-08-01.
- [4] Hugues Chaté and Miguel A. Muñoz. 2014. Insect Swarms Go Critical. *Physics* 7 (2014), 120. <https://physics.aps.org/articles/v7/120>
- [5] Chiara Corbari, Nicola Paciolla, Giada Restuccia, and Ahmad Al Bitar. 2024. Multi-scale EO-based agricultural drought monitoring indicator

- for operative irrigation networks management in Italy. *Journal of Hydrology: Regional Studies* 52 (2024), 101732. doi:10.1016/j.ejrh.2024.101732
- [6] Joshua Fechter. 2021. Texas cities weren't ready for a massive winter storm in 2021. Has that changed? The Texas Tribune. <https://www.texastribune.org/2021/12/06/texas-cities-winter-storm/> Accessed 2025-08-02.
- [7] Anna et al. Florio. 2023. Collaboration is key: Exploring the 2021 flood response for critical infrastructures in Germany. *International Journal of Disaster Risk Reduction* (2023). doi:10.1016/j.ijdr.2023.103710
- [8] Heming Fu, Guojun Xiong, and Shan Lin. 2025. Multi-Agent Reinforcement Learning for Decentralized Reservoir Management via Murmuration Intelligence. *SIGMETRICS Perform. Eval. Rev.* 53, 2 (Aug. 2025), 39–44. doi:10.1145/3764944.3764953
- [9] Prasoon Goyal, Scott Niekum, and Raymond Mooney. 2021. PixL2R: Guiding Reinforcement Learning Using Natural Language by Mapping Pixels to Rewards. In *Proceedings of the 2020 Conference on Robot Learning (Proceedings of Machine Learning Research, Vol. 155)*. PMLR, 485–497. <https://proceedings.mlr.press/v155/goyal21a.html>
- [10] Prasoon Goyal, Scott Niekum, and Raymond J Mooney. 2019. Using natural language for reward shaping in reinforcement learning. In *Proceedings of the Twenty-Eighth International Joint Conference on Artificial Intelligence (IJCAI-19)*. International Joint Conferences on Artificial Intelligence Organization, 2385–2391.
- [11] Sihong He, Songyang Han, Sanbao Su, Shuo Han, Shaofeng Zou, and Fei Miao. 2023. Robust Multi-Agent Reinforcement Learning Considering State Uncertainties. In *Proceedings of the International Conference on Learning Representations (ICLR)*. <https://openreview.net/forum?id=aa4bc40baea2d3d3a7ee416bd5bb9e274bdbe826>
- [12] Sihong He, Songyang Han, Sanbao Su, Shuo Han, Shaofeng Zou, and Fei Miao. 2024. Robust Multi-Agent Reinforcement Learning with State Uncertainty. *Transactions on Machine Learning Research (TMLR)* (2024). <https://openreview.net/forum?id=1sR-7Vuwmy> Accepted. OpenReview: <https://openreview.net/forum?id=1sR-7Vuwmy>.
- [13] H. Hildenbrandt, C. Carere, and C.K. Hemelrijk. 2010. Self-organized aerial displays of thousands of starlings: a model. *Behavioral Ecology* 21, 6 (2010), 1349–1359. doi:10.1093/beheco/arq149
- [14] Jeongwoo Hwang and Upmanu Lall. 2024. Increasing dam failure risk in the USA due to compound rainfall clusters as climate changes. *npj Natural Hazards* 1, 27 (2024). doi:10.1038/s44234-024-00032-5
- [15] J. Kennedy and R. Eberhart. 1995. Particle swarm optimization. In *Proceedings of ICNN'95 - International Conference on Neural Networks*, Vol. 4. IEEE, 1942–1948. doi:10.1109/ICNN.1995.488968
- [16] Ja-Ho Koo, Ali Moradvandi, Edo Abraham, Andreja Jonoski, and Dimitri P. Solomatine. 2025. Flood control of reservoir systems: Learning-based explicit and switched model predictive control approaches. *PLOS Water* 4, 5 (2025), e0000361. doi:10.1371/journal.pwat.0000361
- [17] Brad Lander and New York City Office of the Comptroller. 2024. Is New York City Ready for Rain? An Investigation into the City's Flash Flood Preparedness. <https://comptroller.nyc.gov/reports/is-new-york-city-ready-for-rain/>. Investigation report, New York City Comptroller, April 22 2024.
- [18] Xiang Li, Jiahua Wei, Tiejian Li, Guangqian Wang, and William W.-G. Yeh. 2014. A parallel dynamic programming algorithm for multi-reservoir system optimization. *Advances in Water Resources* 67 (2014), 1–15. doi:10.1016/j.advwatres.2014.01.002
- [19] Nay Myo Lin, Xin Tian, Martine Rutten, Edo Abraham, José M. Maestre, and Nick van de Giesen. 2020. Multi-Objective Model Predictive Control for Real-Time Operation of a Multi-Reservoir System. *Water* 12, 7 (2020), 1898. doi:10.3390/w12071898
- [20] Avery Lotz and Ryan Deto. 2025. Flash flood warnings drench the region. <https://www.axios.com/local/pittsburgh/2025/07/24/flash-flood-warnings-allegheeny-county>. <https://www.axios.com/local/pittsburgh/2025/07/24/flash-flood-warnings-allegheeny-county> Accessed: 2025-08-01.
- [21] Ryan Lowe, Yi Wu, Aviv Tamar, Jean Harb, Pieter Abbeel, and Igor Mordatch. 2017. Multi-Agent Actor-Critic for Mixed Cooperative-Competitive Environments. In *Advances in Neural Information Processing Systems (NeurIPS)*, Vol. 30.
- [22] Yecheng Jason Ma, William Liang, Guanzhi Wang, De-An Huang, Osbert Bastani, Dinesh Jayaraman, Yuke Zhu, Linxi Fan, and Anima Anandkumar. 2023. Eureka: Human-Level Reward Design via Coding Large Language Models. *arXiv preprint arXiv:2310.12931* (2023). <https://arxiv.org/abs/2310.12931>
- [23] Riccardo Poli. 2007. *An Analysis of Publications on Particle Swarm Optimisation Applications*. Technical Report CSM-469. Department of Computer Science, University of Essex. <http://citeseerx.ist.psu.edu/viewdoc/download?doi=10.1.1.75.4036&rep=rep1&type=pdf>
- [24] Tabish Rashid, Mikayel Samvelyan, Christian Schroeder, Gregory Farquhar, Jakob Foerster, and Shimon Whiteson. 2018. QMIX: Monotonic Value Function Factorisation for Deep Multi-Agent Reinforcement Learning. In *International Conference on Machine Learning*. PMLR, 4295–4304.
- [25] Craig W. Reynolds. 1987. Flocks, herds and schools: A distributed behavioral model. In *ACM SIGGRAPH Computer Graphics*, Vol. 21. ACM, 25–34. doi:10.1145/37402.37406
- [26] Michael Rubenstein, Alejandro Cornejo, and Radhika Nagpal. 2014. Programmable self-assembly in a thousand-robot swarm. *Science* 345, 6198 (2014), 795–799.
- [27] Adrian Sainz. 2013. \$2.8B damages in 2011 Mississippi River flood. <https://www.mprnews.org/story/2013/02/25/28b-damages-in-2011-mississippi-river-flood>. Accessed: 2025-08-01. Published by MPR News via Associated Press.
- [28] Margaret M. Sugg, Luke Wertis, Sophia C. Ryan, Shannon Green, Devyani Singh, and Jennifer D. Runkle. 2023. Cascading disasters and mental health: The February 2021 winter storm and power crisis in Texas, USA. *Science of The Total Environment* 880 (2023), 163231. doi:10.1016/j.scitotenv.2023.163231
- [29] Sainbayar Sukhbaatar, Arthur Szlam, and Rob Fergus. 2016. Learning Multiagent Communication with Backpropagation. In *Advances in Neural Information Processing Systems (NeurIPS)*, Vol. 29. <https://arxiv.org/abs/1605.07736>
- [30] Ayoub Tahiri, Daniel Che, David Ladeveze, Pascale Chiron, and Bernard Archimède. 2022. Network flow and flood routing model for water resources optimization. *Scientific Reports* 12, 1 (2022), 3937. doi:10.1038/s41598-022-07969-4
- [31] Mauricio Tec, Guojun Xiong, Haichuan Wang, Francesca Dominici, and Milind Tambe. 2025. Rule-Bottleneck Reinforcement Learning: Joint Explanation and Decision Optimization for Resource Allocation with Language Agents. *arXiv:2502.10732 [cs.LG]* <https://arxiv.org/abs/2502.10732>
- [32] Tamás Vicsek, András Czirók, Eshel Ben-Jacob, Inon Cohen, and Ofer Shochet. 1995. Novel type of phase transition in a system of self-driven particles. *Physical Review Letters* 75, 6 (1995), 1226–1229. doi:10.1103/PhysRevLett.75.1226
- [33] Shen Wang, Ahmad F. Taha, and Ahmed A. Abokifa. 2020. How Effective is Model Predictive Control in Real-Time Water Quality Regulation? State-Space Modeling and Scalable Control. *Water Resources Research* 56, 12 (2020), e2020WR027771. doi:10.1029/2020WR027771
- [34] Guojun Xiong and Milind Tambe. 2025. VORTEX: Aligning Task Utility and Human Preferences through LLM-Guided Reward Shaping. *arXiv:2509.16399 [cs.AI]* <https://arxiv.org/abs/2509.16399>
- [35] Sidney Yakowitz. 1982. Dynamic programming applications in water resources. *Water Resources Research* 18, 4 (1982), 673–696. doi:10.1029/

WR018i004p00673

- [36] Chao Yu, Akash Velu, Eugene Vinitzky, Jiaxuan Gao, Yu Wang, Alexandre Bayen, and Yi Wu. 2021. The Surprising Effectiveness of PPO in Cooperative, Multi-Agent Games. *arXiv preprint* (2021). arXiv:2103.01955 [cs.LG] <https://arxiv.org/abs/2103.01955>
- [37] Chao Yu, Akash Velu, Eugene Vinitzky, Jiaxuan Gao, Yu Wang, Alexandre Bayen, and Yi Wu. 2022. The Surprising Effectiveness of PPO in Cooperative Multi-Agent Games. In *Advances in Neural Information Processing Systems*, Vol. 35. 25072–25085.
- [38] Qian Yu, Yanyan Wang, and Na Li. 2022. Extreme Flood Disasters: Comprehensive Impact and Assessment. *Water* 14, 8 (2022), 1211. doi:10.3390/w14081211
- [39] Kaiqing Zhang, Tao Sun, Yunzhe Tao, Sahika Genc, Sunil Mallya, and Tamer Başar. 2020. Robust Multi-Agent Reinforcement Learning with Model Uncertainty. In *Advances in Neural Information Processing Systems (NeurIPS)*. <https://proceedings.neurips.cc/paper/2020/file/774412967f19ea61d448977ad9749078-Paper.pdf>